NJC

Accepted Manuscript

This is an *Accepted Manuscript*, which has been through the Royal Society of Chemistry peer review process and has been accepted for publication.

Accepted Manuscripts are published online shortly after acceptance, before technical editing, formatting and proof reading. Using this free service, authors can make their results available to the community, in citable form, before we publish the edited article. We will replace this *Accepted Manuscript* with the edited and formatted *Advance Article* as soon as it is available.

You can find more information about *Accepted Manuscripts* in the Information for Authors.

Please note that technical editing may introduce minor changes to the text and/or graphics, which may alter content. The journal's standard Terms & Conditions and the Ethical guidelines still apply. In no event shall the Royal Society of Chemistry be held responsible for any errors or omissions in this *Accepted Manuscript* or any consequences arising from the use of any information it contains.

ROYAL SOCIETY OF CHEMISTRY

www.rsc.org/njc

Journal Name

RSCPublishing

ARTICLE

Reactivity of a Trinuclear Ruthenium Complex Involving C-H Activation and Insertion of Alkene

Cite this: DOI: 10.1039/xoxxoooooox

Zhihong Ma,[a, b] Dong Fan,[a] Suzhen Li,[c] Zhangang Han,[a] Xiaoyan Li,[a,*] Xuezhong Zheng[a] and Jin Lin[a,*]

Received ooth January 2012
Accepted ooth January 2012

DOI: 10.1039/xoxxoooooox

www.rsc.org/

A novel pyridyl-substituted indenyl trinuclear ruthenium complex, $\{\mu_2\text{-}\eta^5:\eta^1\text{-}(C_5H_3N\text{-}6\text{-}Br)(C_9H_5)\}Ru_3(CO)_9$ (**1**) was synthesized by thermal treatment of 1-(6-bromo-2-pyridyl)indene with $Ru_3(CO)_{12}$ (1:1 mol ratio) in refluxing heptane and its reactivity with pyridine derivatives, toluene, indene, fluorene, phenylethylene and divinylbenzene were studied. The reaction of **1** with 5-fold excess of 1-(6-bromo-2-pyridyl)indene gave two products, complex $\{\eta^5\text{-}(C_5H_3N\text{-}6\text{-}Br)(C_9H_5)\}\{\eta^1\text{-}(C_5H_3N)(C_9H_6)\}Ru_2(CO)_4$ **(2)** and substituted dibenzfulvalene (**3**). Reaction of **1** in refluxing toluene obtained an unexpected complex $\{\mu_3\text{-}\eta^6:\eta^3:\eta^1\text{-}(C_5H_3N\text{-}6\text{-}Br)(C_9H_5)\}Ru_3(CO)_7$ **(4)**, via the loss of two CO groups. Reaction of **1** with indene in refluxing heptane afforded a known complex $[\{(\eta^5\text{-}C_9H_7)Ru(CO)_2\}_2]$ **(5)**. The reaction of **1** with fluorene in refluxing heptane afforded complex $\{\mu_3\text{-}\eta^6:\eta^3:\eta^1\text{-}(C_5H_3N\text{-}6\text{-}Br)(C_9H_5)\}Ru_3(CO)_7$ **(4)**, fluorene was not involved in the reaction, indicating that the reaction activity of fluorene is low. The reactions of **1** with phenylethylene or divinylbenzene in refluxing toluene gave the dinuclear ruthenium complexes $\{(\eta^5\text{-}(C_5H_3N\text{-}6\text{-}Br)(C_9H_5CHCH_2Ph\}Ru_2(CO)_5$ **(6)** and $\{(\eta^5\text{-}(C_5H_3N\text{-}6\text{-}Br)(C_9H_5CHCH_2PhCHCH_2\}Ru_2(CO)_5$ **(7)**, respectively. These complexes have been characterized by elemental analysis, IR, and ^1H NMR spectroscopy. The molecular structures of **1**-**6** were determined by X-ray diffraction. The density functional theoretical calculations on the electronic structure of complex **1** give an illustration to its high reactivity.

Introduction

Substituted indenyl anions occupy a prominent role in organometallic chemistry, serving as versatile ligands for transition metals. Seemingly subtle changes in indenyl ligand substitution can have profound consequences on chemical reactivity. The indenyl metal complexes have received increasing attention due to their diverse and flexible hapticities, due to the enhanced reactivity both in stoichiometric and catalytic reactions.[1-9] The indenyl metal complexes containing a donor-functionalized side chain has been receiving much attention.[10-11] For the pyridyl side-chain-functionalized indenyl ligands, the nitrogen atom can act as a good two-electron donor site and can coordinate to a variety of metals, and intramolecular coordination to a Lewis acidic metal center or construction of oligonuclear metal complexes which usually show different structures and reactivities.[12-15] In addition, some cyclopentadienyl metal complexes containing a substituted donor-functionalized side chain and Cp*Ru cluster that C-H activates pyridine have been reported.[16-19] In our previous work we studied the reactions of pyridyl-substituted cyclopentadienes with $Ru_3(CO)_{12}$ and obtained ruthenium carbonyl complexes involving novel intramolecular C-H activation and normal products.[20] By considering the properties and the reactivity of transition-metal complexes are influenced by the electronic and steric properties of the surrounding ligands, we further studied the reaction of pyridyl-substituted indene with $Ru_3(CO)_{12}$ for obtaining deeper insight into the functional group-directed Ru-catalyzed intramolecular aromatic C-H activation and reactivity of the corresponding indenyl metal carbonyl complexes. In this contribution we report the synthesis of pyridyl-substituted indenyl trinuclear ruthenium carbonyl complex $\{\mu_2\text{-}\eta^5:\eta^1\text{-}(C_5H_3N\text{-}6\text{-}Br)(C_9H_5)\}Ru_3(CO)_9$ (**1**) and its reactivity with pyridine derivatives, indene, fluorene, phenylethylene and divinylbenzene. The reactivity of complex **1** and the bonding character of complex **4** are explained based on calculations.

[a]*College of Chemistry & Material Science, Hebei Normal University, Shijiazhuang 050024, China*
[b]*College of Basic Medicine, Hebei Medical University, Shijiazhuang 050017, China*
[c]*Hebei College of Industry and Technology, Shijiazhuang 050091*
Fax: (+86)311-80787431
E-mail: lixiaoyan326@163.com and linjin64@126.com

Experimental

General

Materials

All manipulations of air- and moisture-sensitive complexes were performed at an argon/vacuum manifold using standard Schlenk techniques. All solvents were distilled from appropriate drying agents under an atmosphere of nitrogen prior to use. The ligand precursor 1-(6-bromo-2-pyridyl)indene was synthesized according to the literature.[21]

Equipment and analyses

^{1}H NMR spectra were recorded on a Bruker AV 500 instrument, while IR spectra were recorded as KBr disks on a FT IR 8900 spectrometer. X-ray measurements were made on a Bruker Smart APEX diffractometer with graphite monochromated Mo $K\alpha$ (λ = 0.71073 Å) radiation. Elemental analyses were performed on a Vario EL III analyzer.

Syntheses

Synthesis of 1

A solution of 0.128 g (0.47 mmol) of 1-(6-bromo-2-pyridyl)indene and 0.30g (0.47 mmol) of $Ru_3(CO)_{12}$ in 30mL of heptane was refluxed for 4 h. The solvent was removed under reduced pressure, and the residue was placed in an Al_2O_3 column. Elution with CH_2Cl_2/petroleum ether developed a yellow band, which afforded 0.33 g (84%) of **1** as orange crystals. Mp: 167 ºC. Anal. Calcd for $C_{23}H_8BrNO_9Ru_3$: C, 33.47; H, 0.98; N, 1.70. Found(%): C, 33.45; H, 0.99; N, 1.68. ^{1}H NMR (500 MHz, $CDCl_3$): δ: 7.94 (d, J =8.0 Hz, 1H, Py-H), 7.91 (d, J =8.0 Hz, 1H, Py-H), 7.62 (t, J =7.5 Hz, 1H, Py-H), 7.58 (d, J =8.0 Hz, 1H, C_6H_4), 7.46 (d, J =7.5 Hz, 1H, C_6H_4), 7.32-7.28 (m, 2H, C_6H_4), 5.68 (s, 1H, Cp-H). IR (υ_{CO}, cm^{-1}): 2085(s), 2052(s), 2011(s), 1992(s), 1967(s), 1923(s).

Synthesis of 2 and 3

A solution of 0.223 g (0.27 mmol) of **1** and 0.354 g (1.3 mmol) of 1-(6-bromo-2-pyridyl)indene in 30 mL of heptane was refluxed for 12 h. The solvent was removed under reduced pressure, and the residue was placed in an Al_2O_3 column. Elution with CH_2Cl_2/petroleum ether developed a yellow band and a red band, which gave 0.07 g (22%) of **2** and 0.09 g (26%) of **3** as yellow and red crystals, respectively. Data for **2** are as follows. Mp: 189 ºC. Anal. Calcd for $C_{32}H_{17}BrN_2O_4Ru_2$: C, 49.56; H, 2.21, N, 3.61. Found(%): C, 49.57; H, 2.19, N, 3.60. ^{1}H NMR (500 MHz, $CDCl_3$): δ: 8.14 (d, J =8.0 Hz, 1H, Py-H), 7.99 (d, J =8.5 Hz, 1H, Py-H), 7.69 (d, J =7.5 Hz, 1H, Py-H), 7.60 (t, 2H, Py-H), 7.52 (d, J =8.5 Hz, 1H, Py-H), 7.40-7.36 (m, 1H, Ar-H), 7.37 (d, J =8.0 Hz, 1H, Ar-H), 7.31-7.28 (m, 2H, Ar-H), 7.19 (t, J =7.5 Hz, 1H, Ar-H), 7.08 (t, J =7.5 Hz, 1H, Ar-H), 6.95 (t, J =7.5 Hz, 1H, Ar-H), 6.74 (d, J =7.5 Hz, 1H, Ar-H), 6.38 (s, 1H, Cp-H), 4.36 (d, J =23.0 Hz, 1H, Cp-H), 3.82 (d, J =23.0 Hz, 1H, Cp-H). IR (υ_{CO}, cm^{-1}): 2030(s), 2019(s), 1979(s), 1951(s). Data for **3** are as follows. Mp: 56 ºC. Anal. Calcd for $C_{28}H_{16}Br_2N_2$: C, 62.25; H, 2.99, N, 5.19. Found(%): C, 62.24; H, 3.01 N, 5.18. ^{1}H NMR (500 MHz, $CDCl_3$): δ: 7.95 (t, J =7.5 Hz, 2H, Py-H), 7.92 (d, J =7.5 Hz, 2H, Py-H), 7.90 (d, J =7.5 Hz, 2H, Py-H), 7.63-7.58 (m, 8H, C_6H_4), 5.68 (s, 2H, Cp-H).

Synthesis of 4

(a) A solution of 0.223 g (0.27 mmol) of **1** in 30 mL of toluene was refluxed for 25 h. The solvent was removed under reduced pressure, and the residue was placed in an Al_2O_3 column. Elution with CH_2Cl_2/petroleum ether gave 0.03 g (15%) of **4** as orange-yellow crystals. (b) Using a procedure similar to that described above, reaction of 0.223 g (0.27 mmol) of **1** with 0.216 g (1.3 mmol) of fluorene in 30 mL of heptane also obtained **4** (0.028 g, 14%). Mp: 161 ºC. Anal. Calcd for $C_{21}H_8BrNO_7Ru_3$: C, 32.8; H, 1.05; N, 1.82. Found(%): C, 32.9; H, 1.04; N, 1.75. ^{1}H NMR (500 MHz, $CDCl_3$): δ: 7.42 (t, J =8.0 Hz, 1H, Py-H), 7.20 (d, J =8.0 Hz, 1H, Py-H), 7.03 (d, J =8.0 Hz, 1H, Py-H), 6.18 (t, J =11.0 Hz, 1H, Ar-H), 6.14 (t, J =11.0 Hz, 1H, Ar-H), 4.91 (s, 1H, Cp-H), 4.57 (d, J =11.0 Hz, 1H, Ar-H), 4.54 (d, J =11.0 Hz, 1H, Ar-H). IR (υ_{CO}, cm^{-1}): 2065(s), 1986(s), 1925(s).

Synthesis of 5

Using a procedure similar to that described above, reaction of 0.223 g (0.27 mmol) of **1** with 0.151 g (1.3 mmol) of indene in 30 mL of heptane gave 0.18 g (82%) of **5** as orange yellow crystals. Mp: 224 ºC. Anal. Calcd for $C_{22}H_{14}BrO_4Ru_2$: C, 48.53; H, 2.59. Found(%): C, 48.54; H, 2.58. ^{1}H NMR (500 MHz, $CDCl_3$): δ: 7.31-7.20 (m, 8H, Ar-H), 5.63 (d, J =8.5 Hz, 4H, Cp-H), 5.57 (t, J =7.5 Hz, 2H, Cp-H). IR (υ_{CO}, cm^{-1}): 1940(s), 1774(s).

Synthesis of 6 and 7

A solution of 0.223 g (0.27 mmol) of **1** and 1.3 mmol of phenylethylene or divinylbenzene in 30mL of toluene was refluxed for 4 h. The solvent was removed under reduced pressure, and the residue was placed in an Al_2O_3 column. Elution with CH_2Cl_2/petroleum ether gave the products. Data for **6** are as follows. Orange yellow crystals, yield 0.142g (49%). Mp: 124 ºC. Anal. Calcd for $C_{27}H_{16}BrNO_5Ru_2$: C, 45.28; H, 2.25, N, 1.96. Found(%): C, 45.29; H, 2.24; N, 1.83. ^{1}H NMR (500 MHz, $CDCl_3$): δ: 7.58 (d, J =8.0 Hz, 1H, Py-H), 7.54 (d, J =7.5 Hz, 1H, Py-H), 7.47 (d, J =7.5 Hz, 1H, Py-H), 7.43 (d, J =7.5 Hz, 1H), 7.37-7.35 (m, 2H), 7.32-7.28 (m, 3H), 7.22 (t, J =7.5 Hz, 2H), 7.16 (t, J =7.5 Hz, 1H) (Ar-H), 5.20 (s, 1H, Cp-H), 3.39 (dd, J =15.0, 8.5 Hz, 1H, Ph-CH_2), 3.26 (dd, J =15.0, 6.5 Hz, 1H, Ph-CH_2), 3.06 (dd, J =8.5, 6.5 Hz, 1H, Ru-CH). IR (υ_{CO}, cm^{-1}): 2063(s), 1996(s), 1982(s), 1957(s), 1907(s). Data for **7** are as follows. Orange yellow crystals, yield 0.135g (45%). Mp: 82 ºC. Anal. Calcd for $C_{29}H_{18}BrNO_5Ru_2$: C, 46.91; H, 2.44; N, 1.89. Found(%): C, 46.89; H, 2.45; N, 1.85. ^{1}H NMR (500 MHz, $CDCl_3$): δ: 7.59-7.54 (m, 2H, Py-H), 7.47 (d, J =8.0 Hz, 1H, Py-H), 7.43 (d, J =8.0 Hz, 1H), 7.38-7.29 (m, 3H), 7.26-7.22 (m, 2H), 7.16 (t, J =8.0 Hz, 2H) (Ar-H), 6.70 (dd, J =11.0, 17.5 Hz, 1H, PhCH=CH_2), 5.72 (d, J =17.5 Hz, 1H, PhCH=CH_2), 5.30 (s, 1H, Cp-H), 5.22 (d, J =11.0 Hz, 1H, PhCH=CH_2), 3.37 (dd, J =15.0, 8.5 Hz, 1H, Ph-CH_2), 3.26 (dd, J =15.0, 6.5 Hz, 1H, Ph-CH_2), 3.05 (dd, J =8.5, 6.5 Hz, 1H, Ru-CH). IR (υ_{CO}, cm^{-1}): 2061(s), 1994(s), 1980(s), 1961(s), 1905(s).

Crystal structure determination

Crystals of the complexes **1-6** suitable for X-ray diffraction were isolated from the slow evaporation of hexane-dichloromethane solution. Data collection were performed on a Bruker SMART APEX(□)-CCD detector with graphite monochromated Mo $K\alpha$ (λ = 0.71073 Å) radiation using the φ/ω scan technique. The structures were solved by direct methods and refined by full-matrix least-squares procedures based on F^2 using the SHELX-97 program system. Crystallographic data and experimental details of the structure determinations are given in Table 1. Selected bond lengths and angles are given in Table 2. The single-crystal X-ray determinations are illustrated in Figures 1-6. Crystallographic data for the structural analysis have been deposited with the Cambridge Crystallographic Data Centre, CCDC Nos. 937484, 948153, 1025423, 972419, 968698 and 980936 for **1-6**, respectively. Copies

of this information may be obtained free of charge from The Director, CCDC, 12 Union Road, Cambridge CB2 1EZ, UK, fax: **+44 1223 336 033, e-mail: deposit@ccdc.cam.ac. uk of www: http://www.ccdc.cam.ac.uk.**

Table 1 Crystal data and structure refinement parameters for **1-6**.

	1	**2**	**3**	**4**	**5**	**6**
Empirical formula	$C_{23}H_8BrNO_9Ru_3$	$C_{32}H_{17}BrN_2O_4Ru_2$	$C_{28}H_{16}Br_2N_2$	$C_{21}H_8BrNO_7Ru_3$	$C_{22}H_{14}O_4Ru_2$	$C_{27}H_{16}BrNO_5Ru_2$
Formula weight	825.42	775.53	540.25	769.40	544.47	716.46
Temperature (K)	298(2)	298(2)	298(2)	298(2)	298(2)	298(2)
Crystal system	Triclinic	Monoclinic	Monoclinic	Triclinic	Monoclinic	Monoclinic
Space group	Pī	C2/c	C2/c	Pī	P2(1)/c	P2(1)/c
a (Å)	10.130(3)	24.724(8)	23.277(16)	7.1810(6)	9.241(6)	13.5255(13)
b (Å)	10.886(3)	10.628(4)	6.251(4)	9.6498(8)	13.168(9)	12.8602(9)
c (Å)	11.806(3)	23.593(8)	14.611(11)	16.7441(15)	8.138(6)	15.6149(14)
α (°)	95.962(4)	90	90	95.8890(10)	90.00	90
β (°)	105.519(3)	115.263(4)	92.423(12)	98.2600(10)	112.245(9)	114.691(2)
γ (°)	93.803(3)	90	90	104.031(2)	90.00	90
V (Å^3)	1241.7(6)	5606(3)	2124(3)	1102.52(16)	916.6(11)	2467.7(4)
Z	2	8	4	2	2	4
F (000)	784	3024	1072	728	532	1392
Dcalc (g/cm^3)	2.208	1.838	1.690	2.318	1.973	1.928
Crystal dimensions(mm)	0.27 × 0.18 × 0.08	0.38 × 0.29 × 0.02	0.27 × 0.09 × 0.01	0.15 × 0.12 × 0.10	0.36 × 0.23 × 0.12	0.17 × 0.14 × 0.13
θ Range (°)	1.80-25.50	1.82-25.50	1.75-25.49	2.68-25.02	2.84-25.50	2.65-25.02
Reflections collected	6562	14179	5259	5581	4677	12019
Independent reflections	4539	5217	1980	3822	1701	4350
R_{int}	0.0276	0.0653	0.0551	0.0221	0.0449	0.0498
Parameters	334	370	145	298	128	325
Goodness of fit on F^2	0.986	0.992	0.969	1.046	1.175	1.035
R_1, wR_2 [$I>2\sigma(I)$]	0.0368, 0.0932	0.0417, 0.1015	0.0403, 0.0561	0.0356, 0.0757	0.0327, 0.0842	0.0443, 0.1113
R_1, wR_2 (all data)	0.0446, 0.0967	0.0580, 0.1106	0.0811, 0.0610	0.0572, 0.0871	0.0342, 0.0855	0.0687, 0.1280
CCDC deposition no.	937484	948153	1025423	972419	968698	980936

Table 2 Selected bond distances (Å) and angles (º) for **1-6**.

1	**exp.**	**cal** [a]	**2**		**3**	
Ru(1)-Ru(3)	2.9215(8)	3.013	C(28)-Ru(1)	2.072(5)	Br(1)-C(1)	1.920(3)
Ru(2)-Ru(3)	2.8005(8)	2.872	N(1)-Ru(2)	2.170(4)	C(1)-C(2)	1.376(5)
N(1)-Ru(1)	2.236(4)	2.183	N(2)-Ru(2)	2.270(4)	C(1)-N(1)	1.309(4)
Br(1)-C(14)	1.886(5)	1.915	Br(1)-C(14)	1.887(5)	C(9)-C(10)	1.394(4)
C(8)-Ru(1)	2.054(5)	2.076	C(24)-N(1)	1.389(6)	C(8)-C(8)#1	1.359(6)
Ru(2)-Ru(3)-Ru(1)	81.53(2)	83.3	Ru(2)-C(1)-Ru(1)	115.3(2)	N(1)-C(1)-C(2)	126.8(3)
C(8)-Ru(2)-C(6)	62.34(16)	60.3	C(9)-C(1)-Ru(1)	69.5(2)	C(2)-C(1)-Br(1)	117.9(3)
C(8)-Ru(1)-Ru(3)	78.58(13)	77.8	N(1)-Ru(2)-N(2)	89.10(13)	N(1)-C(1)-Br(1)	115.2(3)
C(22)-Ru(2)-C(23)	91.1(2)	91.9	C(28)-Ru(1)-C(1)	89.91(18)	C(1)-C(2)-C(3)	116.5(3)
C(17)-Ru(1)-C(8)	90.9(2)	91.8	C(28)-N(1)-Ru(2)	125.4(3)	C(8)#1-C(8)-C(7)	127.3(4)
Ru(1)-C(8)-Ru(2)	119.0(2)	118.2	C(14)-N(2)-C(10)	116.0(4)	C(8)#1-C(8)-C(9)	128.8(4)
4	**exp.**	**cal** [a]	**5**		**6**	
Ru(1)-Ru(2)	2.7874(7)	2.818	Ru(1)-Ru(1i)	2.7468(14)	Ru(1)-Ru(2)	2.8192(7)
Ru(1)-Ru(3)	2.9014(8)	2.951	Ru(1)-C(10)	2.061(4)	Ru(2)-N(1)	2.228(5)
Ru(1)-C(2)	2.147(6)	2.161	C(11)-Ru(1)	1.857(4)	Ru(2)-C(15)	2.186(6)
Ru(2)-C(2)	2.037(6)	2.046	C(1)-Ru(1)	2.205(3)	C(15)-C(16)	1.526(8)
Ru(2)-N(1)	2.204(5)	2.261	C(7)-C(8)	1.353(5)	Br(1)-C(1)	1.886(6)
Ru(2)-Ru(1)-Ru(3)	149.77(2)	149.5	Ru(1i)-C(10)-Ru(1)	85.27(12)	C(27)-Ru(2)-Ru(1)	168.11(18)
C(2)-Ru(1)-Ru(2)	46.57(17)	46.2	O(1)-C(11)-Ru(1)	178.4(4)	C(15)-Ru(2)-Ru(1)	79.47(15)
C(2)-Ru(2)-N(1)	79.6(2)	78.5	C(10)-Ru(1)-C(1)	143.07(14)	N(1)-Ru(2)-Ru(1)	87.87(13)
C(14)-N(1)-C(10)	116.3(5)	117.6	C(8)-C(7)-C(6)	121.9(3)	C(1)-N(1)-C(5)	115.8(5)
C(2)-Ru(1)-Ru(3)	104.75(17)	104.7	C(3)-C(2)-C(1)	108.5(3)	C(5)-N(1)-Ru(2)	115.0(4)
C(8)-Ru(3)-Ru(1)	122.0(2)	122.0	C(1)-Ru(1)-Ru(1i)	164.38(11)	C(6)-Ru(1)-Ru(2)	73.64(15)

a: Calculated geometry parameters at B3LYP/ cc-pVDZ-PP level.

Results and Discussion

Reaction of 1-(6-bromo-2-pyridyl)indene with $Ru_3(CO)_{12}$ in heptane

Reaction of ligand precursor 1-(6-bromo-2-pyridyl)indene with $Ru_3(CO)_{12}$ in refluxing heptane afforded the novel trinuclear ruthenium complex, $\{\mu_2\text{-}\eta^5\text{:}\eta^1\text{-}(C_5H_3N\text{-}6\text{-}Br)(C_9H_5)\}Ru_3(CO)_9$ (**1**) in 84% yield (Scheme 1). The formation of complex **1** involves intramolecular C-H bond activation and carbonyl substitution by the pyridyl ligand. Complex **1** could further react with a 5-fold excess of 1-(6-bromo-2-pyridyl)indene to give the dinuclear complex $\{\eta^5\text{-}(C_5H_3N\text{-}6\text{-}Br)(C_9H_5)\}\{\eta^1\text{-}(C_5H_3N)(C_9H_6)\}Ru_2(CO)_4$ (**2**) and substituted dibenzfulvalene (**3**) in 22% and 26% yields, respectively (Scheme 2). The formation of **2** involves the cleavage of C-Br bond. Thermal treatment of **1** in refluxing toluene resulted in the novel complex $\{\mu_3\text{-}\eta^6\text{:}\eta^3\text{:}\eta^1\text{-}(C_5H_3N\text{-}6\text{-}Br)(C_9H_5)\}Ru_3(CO)_7$ (**4**) in very low yield (15%) via the loss of two carbonyl groups (Scheme 3).

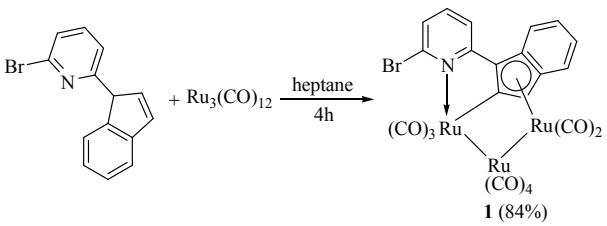

1 (84%)

Scheme 1 Synthesis of **1**

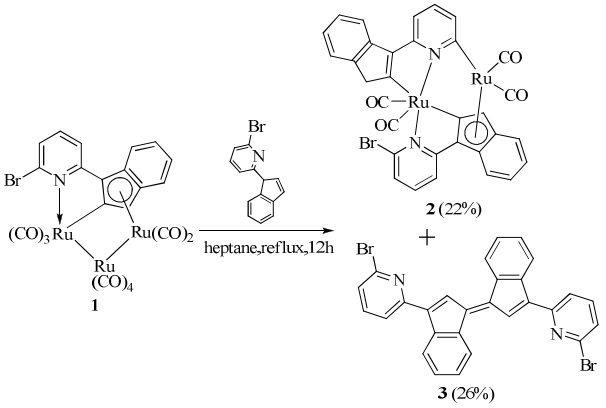

Scheme 2 Synthesis of **2** and **3**

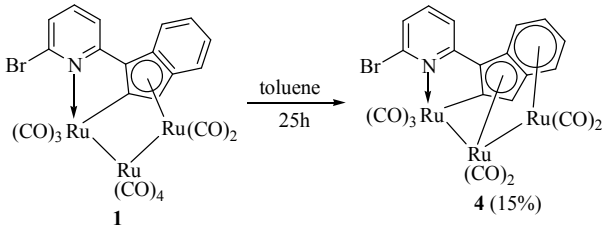

Scheme 3 Synthesis of **4**

A plausible mechanism for the unanticipated formation of **2** is proposed in Scheme 4. First, the N atom of pyridine coordinates to the Ru atom of **1** and replaces one of its CO groups. Then, after intramolecular oxidative addition and reductive elimination a dinuclear ruthenium intermediate is obtained. The final product is finally formed via HBr elimination.

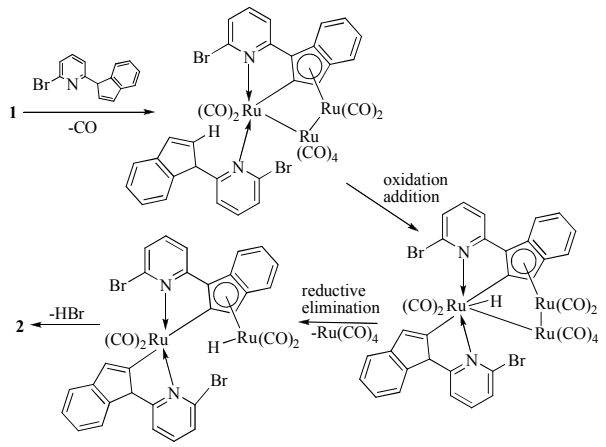

Scheme 4 A plausible mechanism for the formation of **2**

We also wish to propose Scheme 5 to account for the formation of **3**. First, 1-(6-bromo-2-pyridyl)indene undergoes a 1,5-hydride shift process to give its isomer 3-(6-bromo-2-pyridyl)indene. The isomer compound reacts with "$Ru(CO)_4$" species which is produced in the process of generating **2** from **1** to give the bis(η^1-Ind) complex. The intermediate decompose via reductive elimination to give 1,1'-biindene (Ind-Ind). Following by the addition of the benzylic C-H bond of Ind-Ind to the in situ-generated Ru^0 species, (η^1-(1-Ind-Ind))$Ru(CO)_4$(H) is obtained. Finally, β-H elimination of the latter generates Ind=Ind (**3**) and a bis-(hydrido) species that regenerates the original Ru^0 species by eliminating H_2.[22-24]

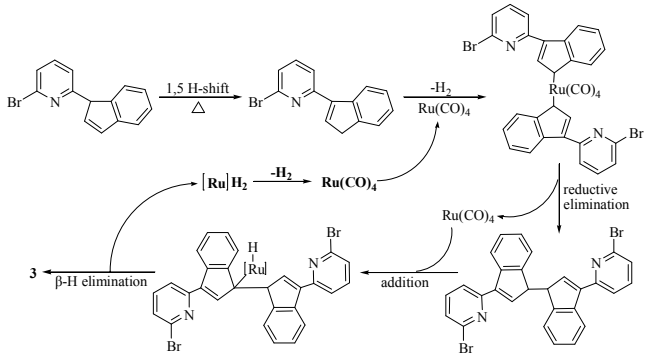

Scheme 5 A plausible mechanism for the formation of **3**

we propose the most likely mechanism for the formation of **4** should involve (i) the initial cleavage of Ru(1)-Ru(3) bond (2.9215(8)Å) of complex **1**, (ii) the subsequent coordination of benzene ring with Ru(3) in η^6 mode via the loss of two carbonyl groups, and (iii) the final coupling of Ru(1)-Ru(2) to form the unexpected complex **4** (Scheme 6).

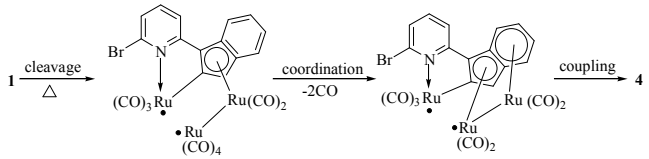

Scheme 6 A plausible mechanism for the formation of **4**

Products **1**-**4** were characterized by ^{1}H NMR, IR, elemental analysis and single-crystal X-ray diffraction analysis (Figures 1-4), and analytical data are in agreement with the structures. In the trinuclear ruthenium complex **1** (Figure 1), the pyridyl indenyl ligand behaves as a tridentate cyclometalated ligand, which forms a coplanar five-membered ring with Ru(1) and also coordinates with Ru(2) in η^5 mode. Both Ru(1) and Ru(2) atoms adopt a pseudooctahedral coordinated mode. The Ru(1)-Ru(3) and Ru(2)-Ru(3) bond lengths are 2.9215(8) and 2.8005(8) Å, respectively. The Ru(1)-C(η^1) distance is 2.054(5) Å, much shorter than those of Ru(2)-C(η^5) (2.215-2.329 Å). In the dinuclear ruthenium complex **2** (Figure 2), both pyridyl indenyl ligands behave as a tridentate ligand, but the coordinated modes of their five-membered ring are different. The one with η^5 and η^1 modes forms a bimetalated cycle including both ruthenium atoms, while the other, with η^1 mode, forms a five-membered cyclometalated ring with Ru(2), as found in complex **1**. The Ru-C(η^1) distances are 2.072(5), 2.099(5) and 2.101(5) Å, respectively, significantly longer than those in **1**. The molecular structure of the trinuclear ruthenium complex **4** (Figure 4) is very novel. The pyridyl indenyl ligand behaves as a tetradentate ligand, and the indenyl unit itself coordinates with three Ru atoms in an unprecedented μ_3-η^6:η^3:η^1-coordinated mode. The Ru(1)-Ru(2) and Ru(1)-Ru(3) bond lengths are 2.7874(7) and 2.9014(8) Å,

respectively, while the Ru(2)-C(η^1) distance is 2.037(6) Å, which are similar to those in **1**.

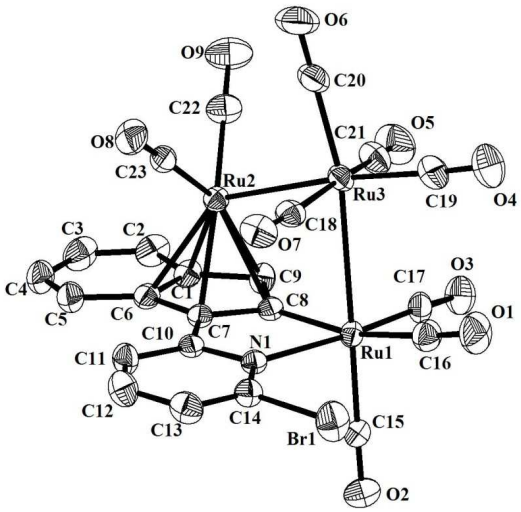

Figure 1 ORTEP diagram of **1**. Thermal ellipsoids are shown at the 30% level. Hydrogen atoms are omitted for clarity.

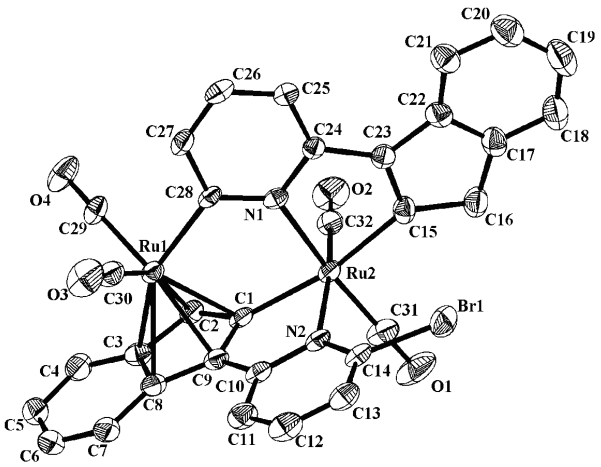

Figure 2 ORTEP diagram of **2**. Thermal ellipsoids are shown at the 30% level. Hydrogen atoms are omitted for clarity.

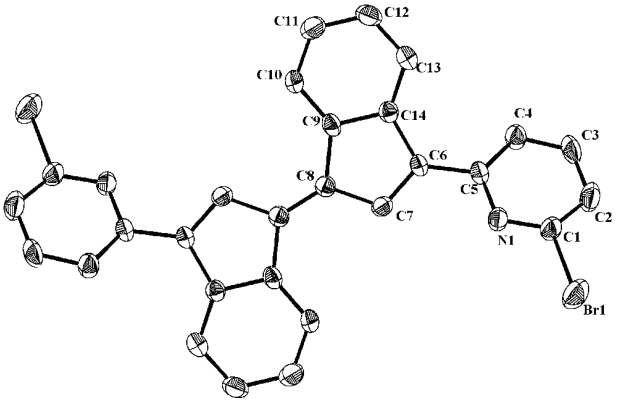

Figure 3 ORTEP diagram of **3**. Thermal ellipsoids are shown at the 30% level. Hydrogen atoms are omitted for clarity.

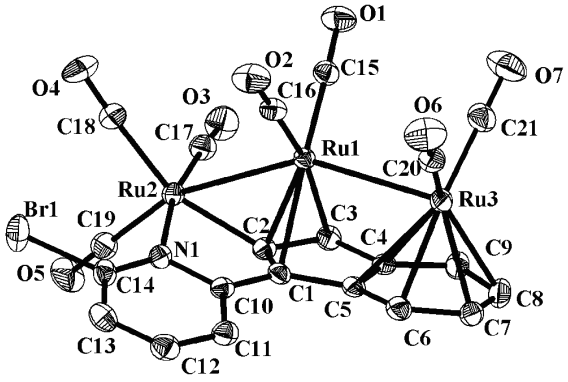

Figure 4 ORTEP diagram of **4**. Thermal ellipsoids are shown at the 30% level. Hydrogen atoms are omitted for clarity.

Reactions of 1 with indene and fluorene

The reaction of indene with **1** in refluxing heptane gave only the known dinuclear ruthenium dimer [{(η^5-C_9H_7)Ru(CO)$_2$}$_2$] (**5**) (Scheme 7). In this reaction we did not observe the formation of complex **4** but afforded a known *trans* Ru-Ru binuclear carbonyl complex **5** (Figure 5) which has higher thermal stability. Its ^{1}H NMR spectra is consistent with the reported value.[25] The Ru-Ru bond length of complex **5** is 2.7468(14) Å, which is very close to the reported value [2.7412(5) Å]. The reaction of fluorene with complex **1** in refluxing heptane is very similar to that of thermal reaction of **1** in refluxing toluene (Scheme 8), complex **4** was obtained in very low yield (13.5%). The formation of **4** involves the cleavage of the Ru-C(η^5) of **1** and the generation of the Ru-C(η^6) and Ru-C(η^3) bonds of **4**. Fluorene was not involved in the reaction, indicating that the reaction activity of fluorene is low, not easy to form complex with metal.

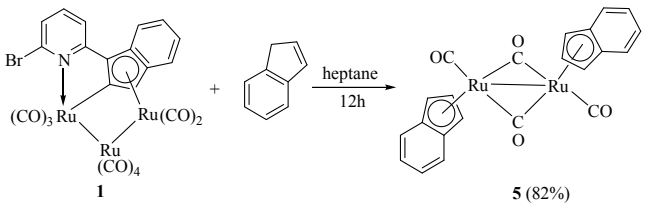

Scheme 7 Synthesis of **5**

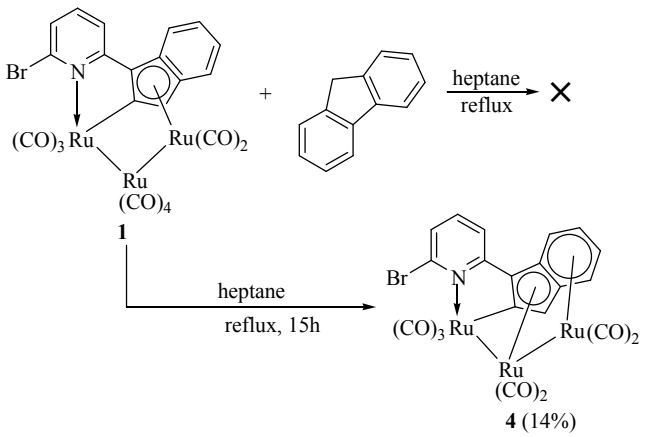

Scheme 8 Synthesis of **4**

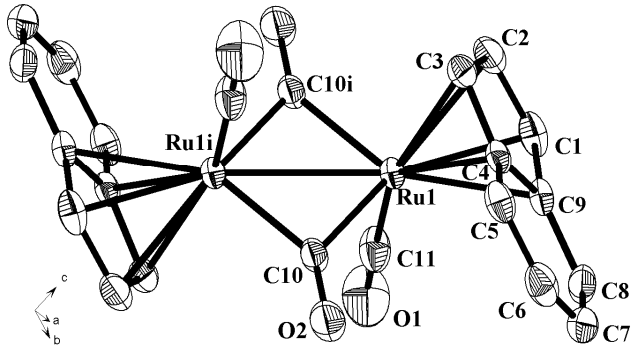

Figure 5 ORTEP diagram of **5**. Thermal ellipsoids are shown at the 30% level. Hydrogen atoms are omitted for clarity. Symmetry code: i: 1-x, -y, -z.

Reactions of 1 with phenylethylene and divinylbenzene

In the above section we have shown that various types of pyridyl ligands are capable of breaking both the Ru-C(η^1) and Ru-C(η^5) bonds of complex **1** to form novel ruthenium complexes. In this section we have investigated the reactivity of **1** with phenylethylene and divinylbenzene. The reactions of **1** with phenylethylene or divinylbenzene in refluxing toluene gave the corresponding dinuclear ruthenium complexes {(η^5-(C_5H_3N-6-Br)($C_9H_5CHCH_2Ph$}$Ru_2(CO)_5$ (**6**) (Scheme 9) and {(η^5-(C_5H_3N-6-Br)($C_9H_5CHCH_2PhCHCH_2$}$Ru_2(CO)_5$ (**7**) (Scheme 10), respectively. Complexes **6** and **7** were formed via the insertion of terminal alkenes into the Ru-C(η^1) bond of complex **1**.[10] Complexes **6** and **7** were characterized by ^{1}H NMR, IR, and elemental analysis. The molecular structure of **6** was further determined by single- crystal X-ray diffraction analysis (Figure 6). The ^{1}HNMR spectra of the alkene-insertion products from terminal alkenes show characteristic resonance, the triplets at 3.05 ppm for Ru-CH protons, indicating a 1, 1-insertion mode. The alkene-insertion reaction generates a new chiral carbon atom σ-bonded to the Ru atom in complexes **6** and **7**, enabling them to exist as a mixture of two isomers theoretically if there are no additional chiral centers in their molecules. However,

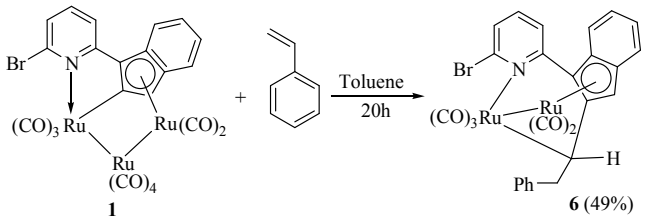

Scheme 9 Synthesis of **6**

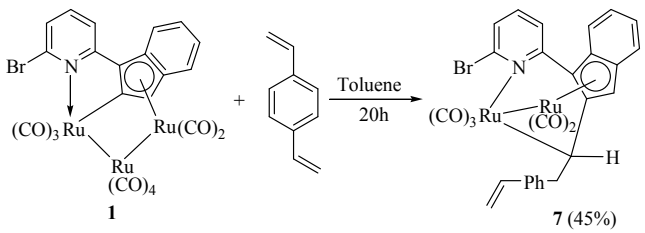

Scheme 10 Synthesis of **7**

there exist only one isomer for complexes **6** and **7**, probably due to the steric effect of the substituents at the chiral carbon. The molecular structure of **6** contains two ruthenium atoms with Ru-Ru bond length of 2.8192(7) Å, an intramolecular coordinated pyridyl, and a cyclometalated unit with the bulky substituent at the chiral carbon deviating away from the pyridyl unit to reduce intramolecular interaction between them. The dihedral angle between the pyridyl ring and the indenyl ring plane is 57.4º.

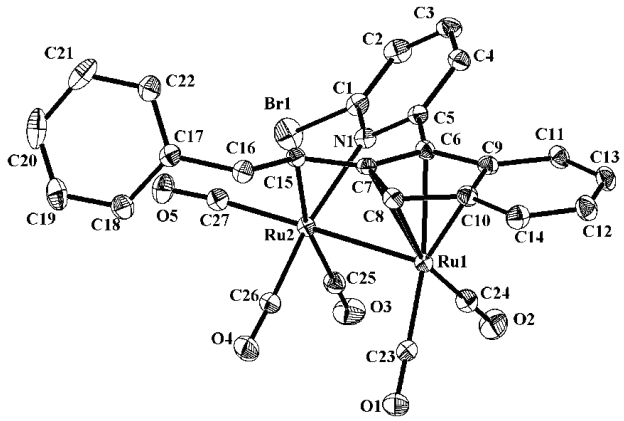

Figure 6 ORTEP diagram of **6**. Thermal ellipsoids are shown at the 30% level. Hydrogen atoms are omitted for clarity.

DFT studies of complex 1 and 4

Computational details

The electronic structures and geometries of complex **1** and **4** were computed by density functional theory (DFT) at the B3LYP level.[26] The C, H, N, O atoms were described using the cc-pVDZ and Ru atoms using cc-pVDZ-PP basis set. The optimized geometries were carried out starting with the geometries found by X-ray crystallography and were characterized as energy minima either by the absence of imaginary frequencies. DFT calculations were performed using the Gaussian 03 suite of programs.[27] The M-M bond orders are calculated through NBO analysis, which was carried out by using the NBO package included in the Gaussian 03 suite of program. The topological structure of complex **4** have been analysis by using the AIM2000 program.[28]

Geometry and reactivity of complex 1

The optimized geometries parameters of complex **1** are also given in Table 2. Cartesian coordinates of the optimized complex **1** are collected in the Supporting Information (Table *S*1). As shown in Table 2, the calculated parameters are very close to the experimental values, which mean that our calculated level is suitable for the study of complex **1**. It is worthy of noticing that the two Ru-Ru bond lengths are different, one is 3.013 (Ru2-Ru3) and 2.872 (Ru1-Ru3) Å. Both of them are longer than twice Pauling's single-bond metal radius (2.50 Å). The wiberg bond order of Ru1-Ru3 and Ru2-Ru3 is 0.4579 and 0.3869. The long Ru-Ru bonds and the bond order indicate that the Ru-Ru bonds in compounds are weak and they are easy to break in reaction. That is, $Ru(CO)_4$ group is active. This conclusion also can be confirmed by the dissociation energies calculations. The dissociation energies calculations of $Ru(CO)_n$(n=2, 3, and 4) are calculated, and the dissociation energy of $Ru(CO)_n$(n=2,

3, and 4) from complex **1** is 213.5, 252.6, and 71.4 kcal/mol, respectively. This means that $Ru(CO)_4$ group is active, it is apt to lost in the reaction than $Ru(CO)_2$ and $Ru(CO)_3$, $Ru(CO)_3$ is the most stable.

Electronic structure of complex 1

A powerful practical model for describing chemical reactivity is the frontier molecular orbital (FMO) theory, developed by K. Fukui in 1950's.[29] The important aspect of the frontier electron theory is the focus on the highest occupied and lowest unoccupied molecular orbital (HOMO and LUMO). The electrons from HOMO orbital are most free to participate in the reaction. Figure 7 gives the HOMO and LUMO orbital of complex **1**. Figure 7 shows that LUMO are mainly contribute by the π orbital of pyridyl and the $Ru(CO)_n$(n=2, 3, and 4). The contribution of Ru1, Ru2, and Ru3 to the LUMO is 19.1%, 6.2%, and 8.5%; The contribution of Ru1, Ru2, and Ru3 to the HOMO is more prominent, it is 14.4%, 27.0%, and 27.7%, respectively. Others FMO (From HOMO-4 to LUMO+4) are shown Figure S1(Supporting Information). It can be seen that most of FMO are contributed by the $Ru(CO)_n$ groups. This means that the $Ru(CO)_n$ groups are the function group of complex **1**. Moreover, the Mulliken charge of Ru1, Ru2, and Ru3 is 0.7484, 0.9277, and 0.2211. Ru3 has the largest positive charge, thus, the electrophile would react with complex **1** at the Ru3 position. It also can be seen that the contribution of Ru2 and Ru3 atom to HOMO is high, especially the Ru3 atom. Therefore, the Ru2-Ru3 bond is easily broken in the reaction and this bond is the reactive site of complex **1** and Ru3 is the active site.

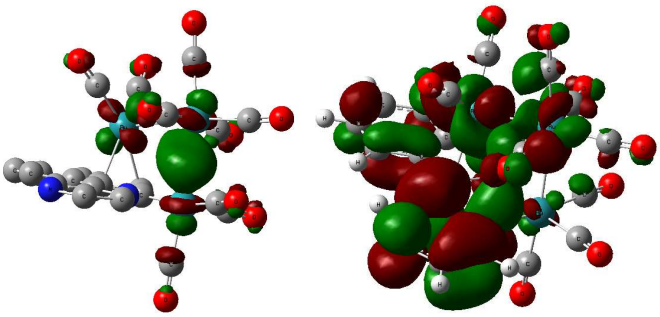

HOMO LUMO

Figure 7 HOMO and LUMO orbitals of complex **1** calculated at B3LYP/ cc-pVDZ level.

Bonding character of complex 4

The optimized geometries parameters of complex **4** are also given in Table 2. Cartesian coordinates of the optimized complex **4** are collected in the Table S2 (Supporting Information). The calculated parameters are very close to the experimental values, too. The bonding of complex **4** is studies by using the "atoms in molecules" (AIM) theory,[30,31] which is proved as a useful tool to study the chemical bonding.[32,33] The molecular graph of complex **4** are shown in Figure 8. There is a bond critical point (BCP) and a pair of bond paths between Ru1 and C1 atom. The existence of the BCP indicates the presence of chemical bond between Ru1 and C2 atom.[30] The similar conditions also existed between Ru3-C6, Ru3-C7, Ru3-C8, Ru3-C9. The molecular graph of complex **4** means that the Ru1 links to one C atom and Ru3 links to four C atoms. Ru1 and Ru3 belong to η^1 and η^4-coordination. The topological properties at the BCP are listed in Table S3 (Supporting Information), which including the electron density ρ_b, the Laplacian of the electron density $\nabla^2\rho_b$, and the total energy density H_b (the sum of the lagrangian kinetic density(G_b) and the virial energy density (V_b)) and the -G_b/V_b. The low ρ_b at the BCP, the positive $\nabla^2\rho_b$ and negative H_b, and $-G_b/V_b$ is between 0.5–1.0 at the BCP mean that the Ru···C bond in these systems are moderately strong, they belong to closed-shell type interaction and have partially covalent shared-closed interaction, according to Cremer's criteria.[30,34]

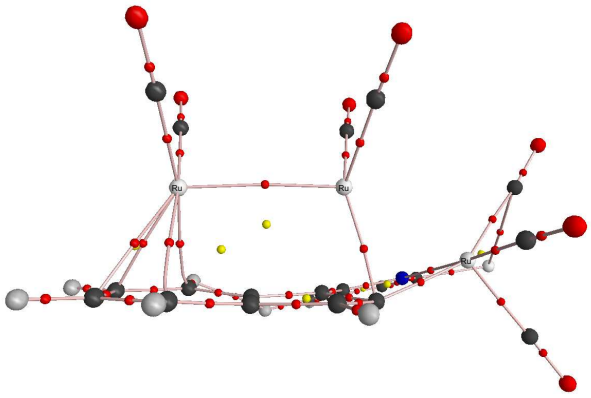

Figure 8 Molecular graph of complex **4** (Small red balls mean BCP and small yellow balls mean RCP).

Conclusions

A novel pyridyl-substituted indenyl trinuclear ruthenium complex, $\{\mu_2\text{-}\eta^5\text{:}\eta^1\text{-}(C_5H_3N\text{-}6\text{-}Br)(C_9H_5)\}Ru_3(CO)_9$ (**1**) was synthesized by thermal treatment of 1-(6-bromo-2-pyridyl)indene with $Ru_3(CO)_{12}$in refluxing heptane and its reactivities with pyridine derivatives, toluene, indene, fluorene, phenylethylene and divinylbenzene were investigated. Our work highlights the diversified reactivity of pyridyl-substituted indenyl ruthenium complexes. We found that complex **1** could be readily converted to the ruthenium complex **2**, in the presence of an excess amount of 1-(6-bromo-2-pyridyl)indene. Thermal treatment of **1** in refluxing toluene generated an unexpected ruthenium complex, $\{\mu_3\text{-}\eta^6\text{:}\eta^3\text{:}\eta^1\text{-}(C_5H_3N\text{-}6\text{-}Br)(C_9H_5)\}Ru_3(CO)_7$ (**4**), by ejecting two carbonyl groups. Complex **4** represents a novel coordination mode ($\mu_3\text{-}\eta^6\text{:}\eta^3\text{:}\eta^1$) of indenyl ligands in transition metal complexes. Reaction of **1** with indene in refluxing heptane afforded a *trans* Ru-Ru dinuclear carbonyl complexes $[\{(\eta^5\text{-}C_9H_7)Ru(CO)_2\}_2]$ (**5**), this shows **1** has higher thermal stability than indene. Reaction of **1** with fluorene in refluxing heptane afforded complex $\{\mu_3\text{-}\eta^6\text{:}\eta^3\text{:}\eta^1\text{-}(C_5H_3N\text{-}6\text{-}Br)(C_9H_5)\}Ru_3(CO)_7$ (**4**), fluorene was not involved in the reaction, indicating that the reaction activity of fluorene is low. Complex **1** reacted with phenylethylene and divinylbenzene to produce the dinuclear complexes **6** and **7** via the insertion of the alkenes into the Ru-C(η^1) bond of **1**. DFT study of complex **1** showed that Ru-Ru bonds in complex **1** are weaken, Ru atom in $Ru(CO)_4$ group has the highest activity and the electrophile group would react at this position; The bonding analysis shows that in complex **4**, Ru1 and Ru3 belong to η^1 and η^4-coordination.

Acknowledgements

This work was supported by the National Natural Science Foundation of China (No. 21372061, 21341003, 21372062, and 21102033), the Hebei Natural Science Foundation of China (Nos. B2013205025 and B2014205018), and the Key Research Fund of Hebei Normal University (No. L2012Z02).

Supplementary information

^{1}H NMR spectra, X-ray coordinates, CIF, CIF checks and DFT computational details for related compounds.

Keywords: indenyl, ruthenium carbonyl, C-H activation, reactivity

Notes and references

1 M. Borah, P. K. Bhattacharyya and P. Das, *Appl. Organometal. Chem*., 2012, **26**, 130.
2 S. Stanowski, K. M. Nicholas and R. S. Srivastava, *Organometallics*, 2012, **31**, 515.
3 Y. Do, J. Han, Y.H. Ree and J. Park, *Adv. Synth. Catal.*, 2011, **353,** 3363.
4 Y. Kuninobu, T. Uesugi, A. Kawata and K. Takai, *Angew. Chem. Int. Ed.*, 2011, **50**, 10406.
5 E. V. Mutseneck, P. V. Petrovskii and A. R. Kudinov, *Russ. Chem. Bull.*, 2004, **53**, 2090.
6 D. Zargarian, *Coord. Chem. Rev.*, 2002, **157**, 233.
7 M. J. Calhorda, V. Félix and L. F. Veiros, *Coord. Chem. Rev.*, 2002, **230**, 49.
8 M. Stradiotto and M. J. Mcglinchey, *Coord. Chem. Rev.*, 2001, **219-221**, 311.
9 L. Resconi, L. Cavallo, A. Fait and F. Piemontesi, *Chem. Rev*,. 2000, **100**, 1253.
10 D. Chen, X. Zhang, S. Xu, H. Song and B. Wang, *Organometallics*, 2010, **29**, 3418.
11 D. Chen, C. Zhang, S. Xu, H. Song and B. Wang, *Organometallics*, 2011, **30**, 676.
12 P. J. Fischer, K. M. Krohn, E. T. Mwenda and V. G. Jr. Young, *Organometallics*, 2005, **24**, 1776.
13 C. Müller, D. Vos and P. Jutzi, *J. Organomet. Chem.,* 2000, **600**, 127.
14 U. Siemeling, *Chem. Rev.*, 2000, **100**, 1495.
15 H. Butenschon, *Chem. Rev.*, 2000, **100**, 1527.
16 D. Chen, Y. Li, B. Wang, S. Xu and H. Song, *Organometallics*, 2006, **25**, 307.
17 N. C. Ackroyd and J. A. Katzenellenbogen, *Organometallics*, 2010, **29**, 3669.
18 J. Okuda and K. H. Zimmermann, *Chem*. *Ber*., 1989, **122**, 1645.
19 T. Takao, T. Kawashima, H. Kanda, R. Okamura and H. Suzuki, *Organometallics*, 2012, **31**, 4817.
20 J. Lin, Z. H. Ma, F. Li, M. X. Zhao, X. H. Liu and X. Z. Zheng, *Transition Met. Chem.*, 2009, **34**, 855.
21 D. Chen, S. Xu, H. Song and B. Wang, *Eur. J. Inorg. Chem.*, 2008, 1854.
22 C. Sui-Seng, G. D. Enright and D. Zargarian, *J. Am. Chem. Soc*., 2006, **128**, 6508.
23 A. Jończyk, P. Szymanek and C. Juszczuk, *Polish J. Chem.*, 2000, **74**, 985.
24 A. G. Anastassiofu, L. Setliff and G. W. Griffin, *J. Org. Chem.*, 1966, **31**, 2705.
25 V. S. Sridevi and W. K. Leong, *J. Organomet. Chem.,* 2007, **692**, 4909.
26 (a) C. Lee, W. Yang and R. G. Parr, *Phys. Rev. B.,* 1988, **37**, 785. (b) A. D. Becke, *J. Chem. Phys.*, 1993, **98**, 5648.
27 M. J. Frisch, G. W. Trucks, H. B. Schlegel, G. E. Scuseria, M. A. Robb, J. R. Cheeseman, J. A. Jr. Montgomery, T. Vreven, K. N. Kudin, J. C. Burant, et al. Gaussian, Inc.: Wallingford CT, 2004.
28 F. Biegler-König, AIM 2000, Version 1.0; University of Applied Science: Bielefeld, Germany, 2000.
29 F. Kenichi, Y. Teijiro and S. Haruo, *J. Chem. Phys.*, 1952, **20**, 722.
30 R. F. W. Bader, Atoms in Molecules: A Quantum Theory, Oxford University Press: Oxford, 1994.
31 P. Popelier, Atoms in Molecules: An Introduction, Prentice Hall: Manchester, 2000.
32 X. Y. Li, S. H. Huo, Y. L. Zeng, Z. Sun, S. J. Zheng and L. P. Meng, *Organometallics*, 2013, **32**, 1060.
33 F. F. Lu, X. Y. Li, Y. L Zeng, X. Y Zhang and L. P. Meng, *New J Chem.*, 2014, DOI: 10.1039/c4nj00918e.
34 D. Cremer and E. Kraka, *Angew. Chem. Int. Ed. Engl.*, 1984, **23**, 627.

